

Comparison of Three Methods to Obtain the Apparent Dielectric Constant from Time Domain Reflectometry Wave Traces

D. J. Timlin* and Ya. A. Pachepsky

ABSTRACT

A calibration of time domain reflectometry (TDR) probes to measure soil water in a particular soil is desirable since no consistent relationship between water content and apparent dielectric constant (K_a) has been found. We compared three procedures to compute K_a from TDR traces: a manual method that uses a plot of the wave trace, a derivative-based computer algorithm, and fitting a simulated TDR trace to a measured one with a simple multiple reflection model. We added a model of inertia to the multiple reflection model to approximate the rise time of the cable tester. The TDR traces were measured in situ with a Tektronix 1502B cable tester (Tektronix, Inc., Wilsonville, OR) on samples from two soils with contrasting textures, Beltsville silt loam (fine-loamy, mixed, mesic Typic Fragiudult) and Rumford loamy sand (coarse-loamy, siliceous, thermic Typic Normudult). Ten-centimeter probes with three rods were used. The water contents were measured gravimetrically with soil cores. Calibration with apparent dielectric constants obtained from the derivative-based algorithm had the smallest standard error for both soils, and the manual method was better than the wave simulation method. The intercepts and slopes of the calibration equations for the manual and derivative methods were not significantly different from each other for both soils. The wave simulation method, which gives physically meaningful values for K_a , and characteristic impedances can be a useful tool for theoretical studies.

TIME DOMAIN REFLECTOMETRY has become a popular method to measure water content in soils. The method is quick, reproducible, and has a sound theoretical basis. The TDR measurement technique is based on the estimate of the time needed for an electromagnetic pulse to travel along metal rods (waveguides) inserted into the soil. The travel time depends on the apparent dielectric constant (K_a) of the three-phase soil system. A calibrated relationship between travel time (a function of K_a) and soil water content (θ) is needed to use TDR for measurements of soil water content.

The calibration of TDR can be done in a laboratory using soil cores with controlled water content. Carefully packed soil cores are generally used for this purpose (Ledieu et al., 1986; Dirksen and Dasberg, 1993). Alternatively, measurements can be done in the field and cores can be taken to represent the soil volume surrounding the TDR waveguides.

Topp et al. (1980) reported a strong relationship between K_a and soil volumetric water content for a wide range of soils. This relationship was found to apply to other soils in later tests as well (Dalton and van Genuch-

ten, 1986; Zegelin et al., 1989). Other authors, however, reported relationships that differed from Topp et al. (1980) for the soils in their studies (Dasberg and Hopmans, 1992; Herkelrath et al., 1991; Dobson et al., 1985). The presence of organic matter, influence of clay content, and soil structural complexity were mentioned by these authors as possible factors influencing the K_a (θ) relationship for a particular soil. Jakobsen and Schønning (1993a), however, encountered statistically significant differences in calibration relationships among soil types that could not be explained by differences in bulk density and texture.

Since TDR has a high spatial resolution (Knight, 1992; Baker and Lascano, 1989), the presence of macropores, rocks, root channels, and large aggregates may influence field TDR measurements (Jakobsen and Schønning, 1993b). Field TDR data can also reflect variations of soil water content along the waveguides (Dasberg and Hopmans, 1992). Because of these reasons, field measurements are important for TDR calibrations since the effect of small-scale soil heterogeneity may be incorporated into the calibration curves.

While the measurement and recording of TDR signals can be easily automated, the method by which the travel time is obtained from the wave trace is more cumbersome and can be a source of error for TDR measurements (Topp et al., 1980; Dasberg and Hopmans, 1992). In their study, Topp et al. (1980) noted that the major source of uncertainty in the calibration of TDR was from the measurement of travel time from photographs of the wave traces.

The K_a of the soil is a function of the travel time of the electromagnetic pulse along the waveguides. There are two common methods to obtain this travel time from a recorded signal trace: (i) measuring the signal trace manually, and (ii) a computer algorithm to find the initial and end points of the trace by searching for characteristic slope changes. A third method, proposed by Yanuka et al. (1988), is an inverse approach to obtain the parameters of the transmission line system from the wave trace. It is based on the simulation of the wave propagation using a theoretical description of voltage reflections.

The usefulness of the Yanuka et al. (1988) method has never been fully investigated or compared with the other two methods. The objective of this paper was to compare these methods of reflection pattern analysis to calibrate a TDR probe using field measurements.

MATERIALS AND METHODS

Time Domain Reflectometry Trace Analysis

An ideal trace for the propagation of a voltage pulse in a three-piece transmission line cable-handle-waveguide, which

D. J. Timlin, USDA-ARS, Systems Research Lab., Bldg. 007, Rm. 008, BARC-West, Beltsville, MD, 20705; and Ya. A. Pachepsky, Dep. of Botany, Duke Univ., Durham, NC 27708. Ya. A. Pachepsky is on leave from the Inst. of Soil Science and Photosynthesis, Pushchino, 142292, Russia. Received 14 Mar. 1995. *Corresponding author (dtimlin@ars.arsusda.gov).

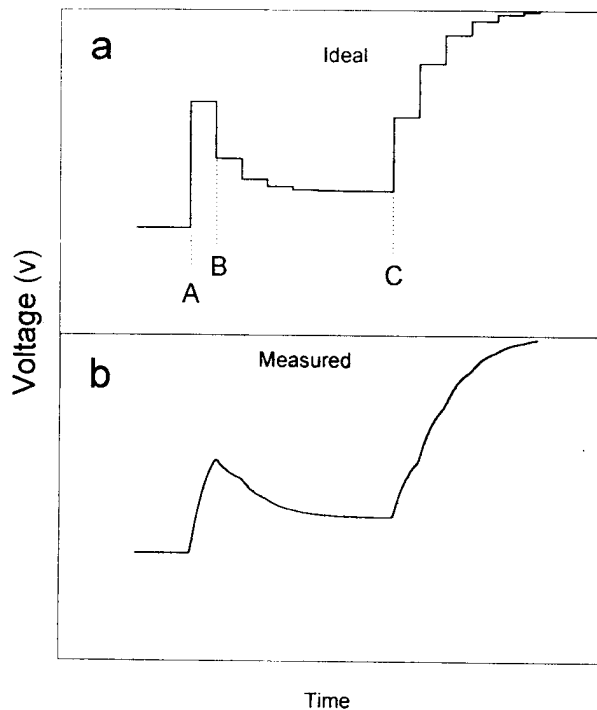


Fig. 1. Voltage reflections from a cable tester showing (a) an ideal representation of the wave trace and (b) a wave trace for a probe in soil.

is typical for measurements in soils, is shown in Fig. 1a. The rectangular wave above the interval AB is caused by the reflection from the cable-handle connection, travel along the handle and, then reflection from the handle-waveguide connection. The rising signal beginning at C is caused by the reflection from the ends of the waveguides. For times larger than C, the trace pattern is a result of multiple reflections from the handle and waveguides. The length BC is proportional to the travel time in the soil and to K_a . The travel time in the soil can be converted to an equivalent distance L_{BC} by using the relative velocity of propagation (V_p) setting of the time domain reflectometer or cable tester. The velocity of propagation is the ratio of the velocity (v) of electricity in a cable or waveguide compared with the velocity (c) of electricity traveling in a vacuum. Here, c is the speed of light. In practice, when the cable tester is used to measure K_a of soils, V_p is set at the highest level, 0.99. The length of the waveguides as measured by the cable tester is then longer than the physical length of the waveguides if $K_a > 1$. With the following relationships

$$\sqrt{K_a} = \frac{c}{v}; \quad v = \frac{2L}{t_{BC}}; \quad [1]$$

it can be shown that

$$K_a = \left(\frac{L_{BC}}{L}\right)^2 \quad [2]$$

where L is the physical length of the waveguide, c is the speed of light, and L_{BC} is the electrical length of the probes recorded by the cable tester, which is equal to ct_{BC} . The distance L_{BC} can be physically measured from the wave trace when the x axis is given in units of distance.

The goal of wave trace analysis is to find the boundaries of the reflections at Points B and C in Fig. 1a, to determine

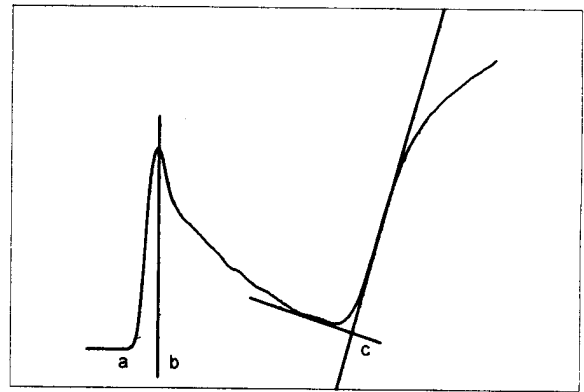


Fig. 2. Manual method to obtain the dielectric constant of wet soil.

the travel time, and hence L_{BC} , as represented by the length BC. The analysis requires a procedure that approximates an ideal FDR trace from a measured trace with dispersion. A wave trace measured by a cable tester in a soil with the same K_a as the ideal transmission line of Fig. 1a is shown in Fig. 1b. The measured traces are rounded by dispersion because of the measurement delay of the instrument and nonideal behavior of the soil, the dielectric medium, and the probe and cable. The degree of dispersion increases with longer cables and number of reflections (Heimovaara, 1993). Variations in soil water content along the rods may also contribute to dispersion. Dispersion controls the precision of the instrument and limits the use of short waveguides. The differences between the shapes of the measured and ideal traces complicate the problem of determining the length (L_{BC}) of the waveguides in soil.

The manual method used for this paper illustrated by Fig. 2 is also described in Topp et al. (1982). The location of the handle is generally identified at the peak of the steeply rising line. However, the selection of this point is largely determined by the characteristics of the probe and the resultant wave trace. The one important requirement is that this point be easy to recognize and have a consistent location in the wave trace. Leduc et al. (1986) used a probe that had diodes installed in the handle; the resultant impedance mismatch gave a characteristic valley in the initial part of the wave trace. A line is drawn parallel with the Y axis through the peak and the location of the intersection of this line with the X axis is designated as b in Fig. 2. This corresponds to Point B in Fig. 1a. Point C is located at the intersection of two lines drawn tangent to the curve at the positions shown.

The numerical differentiation method described next had been proposed by Baker and Allmaras (1990) and modified in Spaans and Baker (1993). This method is essentially an adaptation of the manual method to automate the calculation of travel times from TDR wave traces. We used Spaans and Baker's source code for the calculations.¹ The program was modified by us to read input files that have a different format and output values of K_a rather than water content. The method is illustrated in Fig. 3. The measured trace is smoothed numerically (Fig. 3a) and the first derivative (slope) is calculated (Fig. 3b). The point on the smoothed trace at the maximum derivative is the first inflection point. It is assumed here that the reflection off the handle has the steepest slope. A line through the mean of the first seven points of the smoothed curve is drawn parallel to the X axis. A line tangent to the inflection point is drawn

¹ The source code was obtained from Midwest Special Services, 900 Ocean St., St. Paul, MN 55106.

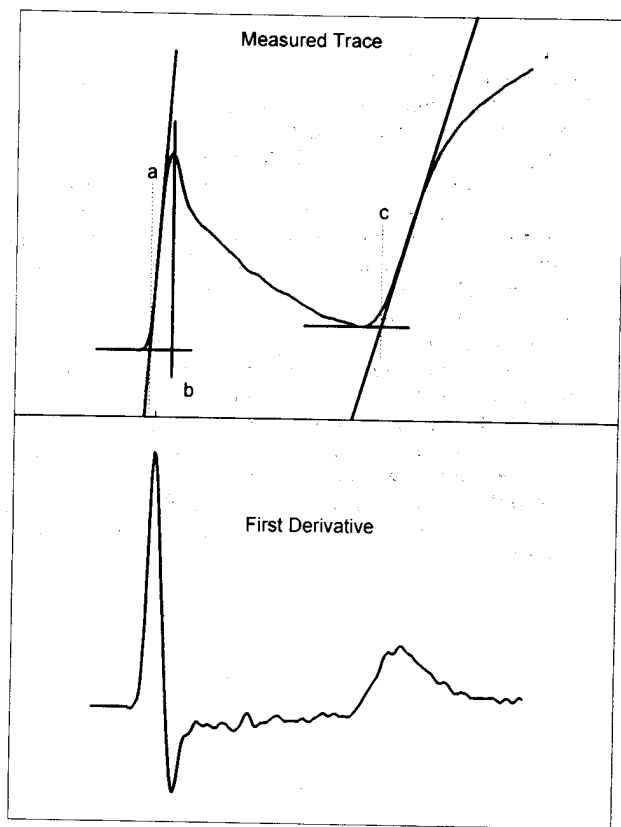


Fig. 3. Derivative-based method to obtain the dielectric constant of wet soil.

to intersect this line and the intersection point is *a*, corresponding to Point A on the ideal trace in Fig. 1a. A probe constant to account for the apparent length of the probe handle is added to *a* to obtain *b* (Fig. 3a), which corresponds to Point B in Fig. 1a. The program next searches the smoothed trace (Fig. 3a) for a local minimum in a region that begins at a distance from the handle of 0.8 times the length of the waveguide and ends at the location of the next maximum first derivative. A line parallel to the X axis is drawn tangent to this local minimum. A second tangent is placed at the point of the second maximum of the first derivative following the local minimum. The intersection of this line with the horizontal line is Point *c* (Fig. 3a), which is equivalent to Point C in Fig. 1a. In a very dry soil where the slope of the trace does not decrease after the initial inflection (Point *b*), a different approach is used to find the second inflection point.

The third method is based on a simple and efficient multiple reflection technique proposed by Yanuka et al. (1988) to predict an ideal trace for a composite transmission line using the electromagnetic parameters of each section of the line. The following assumptions are made for this method: (i) The soil is a nonconductive dielectric medium. This assumption means that there is no attenuation of the wave trace, i.e., the final voltage is twice the initial voltage. This assumption will not result in large errors in soils with low conductivities. Furthermore, the conductivity of the soil has little effect on the travel time along the waveguides (Topp et al., 1980). While this assumption may result in slightly more error, the advantage is that the number of parameters to be fit is less. (ii) Each homogeneous section of the transmission line, i.e., cable, handle, and waveguides (rods) can be characterized by three parameters: impedance Z_s , the apparent dielectric constant K_s of the surrounding medium, and the length of the section L . (iii) For the given set of electromagnetic parameters, the TDR

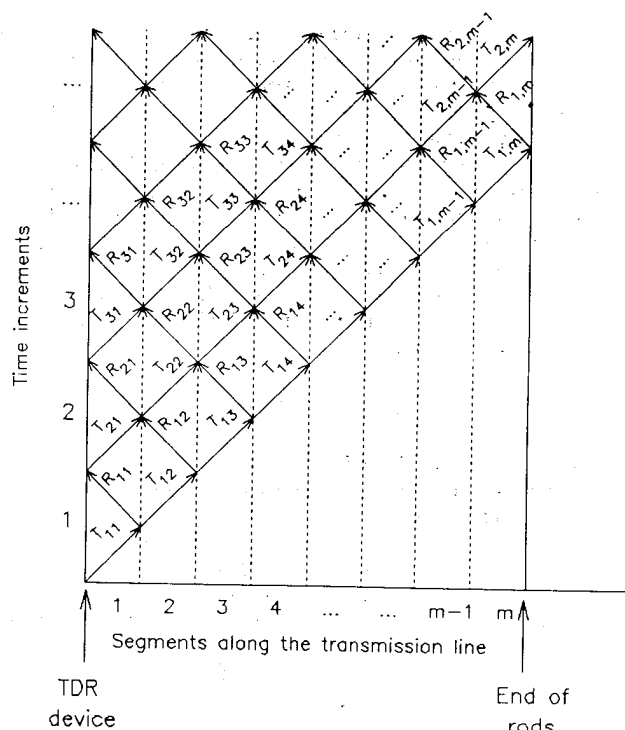


Fig. 4. The transmission and reflection of voltages that contribute to the voltage at a particular time. $R_{i,j}$ are reflected voltages and $T_{i,j}$ are transmitted voltages at time i and node j (TDR = time domain reflectometry).

trace can be simulated with the technique of Yanuka et al. (1988).

The general idea of the method is to choose parameters of the transmission line sections that provide the best correspondence between the measured and simulated trace. To simulate a trace with the multiple reflection model, one has to subdivide the transmission line into small segments and to calculate reflected and transmitted voltages at the segment boundaries for a sequence of time increments. Reflected voltages that return to the voltage propagation source are accumulated for each value of time, and the simulated TDR trace is the summation of the accumulated voltages as a function of time.

The lengths of the segments along the transmission line are selected to allow the wave to pass the segment twice during one time increment. Segments have uniform length within a homogeneous section of the transmission line (i.e., cable, handle, and waveguides), and the segment length varies from one section to another, since the velocity of the wave propagation differs. The total number of segments within a section k is calculated as

$$N_k = \frac{2L_k}{\frac{c}{\sqrt{K_{sk}}}\Delta t} \quad [3]$$

Here, L_k is the length of the section, $(K_s)_k$ is the apparent dielectric constant of the section, and c is the speed of light. The time step, Δt , is chosen to provide sufficiently fine discretization of the transmission line. In this equation, N_k is truncated to an integer.

Figure 4 depicts a wave propagation pattern used in the method. The first subscript in Fig. 4, denoted as i in the equations, denotes the time increment, and second subscript j refers to the segment number. Reflected and transmitted voltages are traced in each segment beginning at the time when the pulse sent by the cable tester reaches the boundary of the

segment. Within each time increment, the transmitted voltage, $T_{i,j}$ heading toward the end of the transmission line (i.e., the end of rods) and the reflected voltage, $R_{i,j}$ heading toward the beginning of the transmission line [i.e., to the cable tester pass the segment (Fig. 4)].

The reflection coefficient (ρ) is used to establish the relationship between reflected and transmitted voltages. When a voltage pulse, V , moving from $j - 1$ to j passes a boundary between two segments $j - 1$ and j , the reflected voltage is equal to $\rho_{j-1,j}V$, and transmitted voltage is $(1 + \rho_{j-1,j})V$ where $\rho_{j-1,j}$ is the reflection coefficient between Segments $j - 1$ and j depending on the characteristic impedances, Z_s , of the two neighboring segments:

$$\rho_{j-1,j} = \frac{Z_{s(j-1)} - Z_{s(j)}}{Z_{s(j-1)} + Z_{s(j)}} \quad [4]$$

where $Z_s = Z_0/K_a^{0.5}$, and Z_0 is an impedance of the segment that does not depend on the dielectric properties of the medium surrounding the segment. Within the network of transmitted and reflected voltages in Fig. 4, two voltage pulses $T_{i,j-1}$ and $R_{i-1,j}$ come to the left boundary of Segment j in the beginning of the time increment I . The two voltages are both reflected and transmitted, and the voltage pulses $T_{i,j}$ and $R_{i,j-1}$ are formed as a result. The value of $T_{i,j}$ is the result of the transmission of voltage $T_{i,j-1}$ from $j - 1$ to j and of the reflection of voltage $R_{i-1,j}$ back to j . Therefore

$$T_{i,j} = (1 + \rho_{j-1,j})T_{i,j-1} - \rho_{j-1,j}R_{i-1,j} \quad [5]$$

here $\rho_{j-1,j} = -\rho_{j,j-1}$ is used. The value of $R_{i,j-1}$ is the result of the transmission of voltage $R_{i-1,j}$ from Segment j to $j - 1$ and of the reflection of voltage $T_{i,j-1}$ back to $j - 1$. Therefore

$$R_{i,j-1} = (1 - \rho_{j-1,j})R_{i-1,j} + \rho_{j-1,j}T_{i,j} \quad [6]$$

The value of $\rho_{j-1,j}$ is equal to 0 if the Segments $j - 1$ and j belong to the same homogeneous section of the transmission line. Therefore, within homogeneous segments, $T_{ij} = T_{i,j-1}$ and $R_{i,j-1} = R_{i-1,j}$.

Separate equations are used to define the transmitted and reflected voltages at the boundaries of the network. At the cable tester, the first transmitted voltage $T_{1,1}$ is equal to the voltage pulse of the TDR, V_0 . After the first voltage pulse, all transmitted voltages $T_{i,1}$ for later time steps are equal to zero because the device no longer sends out voltages. At the first time step, it is assumed there are no incoming reflections, i.e., $R_{0,j} = 0$. At the end of the waveguides ($j = m$), ideal reflection is assumed and $\rho_{m,m+1} = 1$.

Calculations of multiple reflections and transmissions are carried out with Eq. [5] and [6]. For each time increment $I = 1, 2, \dots$, Eq. [5] is applied for each $j = 1, 2, \dots, m - 1$ to find T_{ij} , and then Eq. [6] is used for each $j = 1, 2, \dots, m - 1, m$ to obtain $R_{i,j}$. At the end of each increment, the resulting voltage at the cable tester is accumulated as $V = V + R_{i,1}$.

The parameters, K_a and Z , of the handle and rods are chosen to provide the best correspondence between measured and simulated wave traces. The parameters for the cable are known and do not need to be fit. We applied a modified Marquardt-Levenberg algorithm to minimize the sum of squared differences between the calculated and measured voltages. We used a version of the algorithm published by van Genuchten (1981), which proved to be very efficient in multi-parametric nonlinear minimization. To avoid local minimums, we made 100 runs for every sample with random selections of initial parameter estimates. The parameters that gave the smallest error were then used as initial conditions for the minimization step.²

The multiple reflection model described above will produce

an ideal trace similar to the trace in Fig. 1a. The nonlinear optimization method may yield poor estimates of the parameters because the angular shapes of the ideal traces differ markedly from the smooth measured wave form shown in Fig. 1. In their paper, Yanuka et al. (1988) noted poor correspondence with measured data in some cases. They concluded that the poor fit was because the model did not account for relaxation or dispersion phenomena in the medium and that it may not account for all reflections. They also concluded that the measurement delay of the cable tester may result in a loss of information for some sections of the signal.

Time Domain Reflectometry instruments have a rise time, which is the time required for the measured voltage to go from 10% to 90% of its maximum amplitude. The rise time of the TDR accounts for a part of the rounding of the wave trace. Because this rise time can be considered to result from a type of inertia, we added a model of inertia of the cable tester to the model of Yanuka et al. (1988) to improve the fit.

An ideal registering device integrates reflections $R(t)$, which are derivatives of the incoming voltage:

$$V = \int_0^t R(\tau) d\tau + V_0 \quad [7]$$

Here V is the registered voltage and V_0 is the initial voltage. Equation [7] is equivalent to

$$\frac{dV}{dt} = R(t) \quad [8]$$

In the transmission line cable-handle-waveguide, the reflections are discrete needle-shaped voltage jumps, and their integration in Eq. [7] creates the angular form of the trace as shown in Fig. 1a. Assuming that the inertia acts in proportion to the derivative of the voltage rise rate, we replaced Eq. [8] by the equation

$$\lambda \frac{d^2V}{dt^2} + \frac{dV}{dt} = R(t) \quad [9]$$

The deviation of the signal from an ideal one is governed by the value of the parameter λ , which will be called the characteristic inertia time. The effect of λ in Eq [9] is to cause the voltage rise to slow down. The damping effect will be greater as the rate of voltage rise increases, i.e., the faster the voltage rises, the more it is damped. Equation [9] with initial conditions $V(0) = 0$ and $dV/dt|_0 = 0$ has the following solution (using the method of reduction of order):

$$V(t) = \frac{1}{\lambda} \int_0^t \left\{ \int_0^\tau R(s) \exp\left(\frac{s}{\lambda}\right) ds \right\} \exp\left(-\frac{\tau}{\lambda}\right) d\tau \quad [10]$$

which we used to integrate incoming reflections calculated by the model of Yanuka et al. (1988). Here $R(s)$ is the voltage that is reflected back to the source, and s and τ are dummy variables of integration that refer to time. In the program, Eq. [10] is numerically integrated using trapezoid integration over two values of the function. The parameter λ was included into the set of parameters to be found from the optimization with the dielectric constants and impedances of the handle and waveguides. We first ran simulations to fit λ for each wave trace. The final simulations were carried out with a mean value of λ from these initial simulations.

For each of the three methods, we assumed the K_a (θ) relationship could be described by the equation reported by Ledieu et al. (1986) wherein water content is a linear function of $K_a^{0.5}$ (or L_a/L). The coefficients of the calibration equations were compared by using Proc Reg of SAS (SAS Institute, 1985). We used indicator variables (Neter and Wasserman, 1974, p. 279-338) in multiple linear regression to obtain

² The program, coded in FORTRAN, is available from the authors upon request.

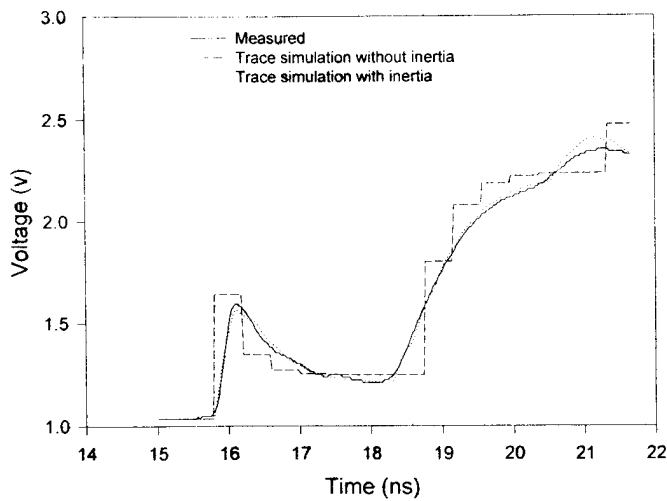


Fig. 5. Measured and fitted time domain reflectometry traces for the transmission line consisting of a cable, a handle, and waveguides in soil.

parameters for all methods to calculate values of the Students *t*-statistic to make comparisons.

Experimental Data

Measurements were collected in field soil with a balanced probe that had three 10-cm-long rods 0.3175 cm (1/8 in.) in diameter as waveguides, and the distance between the outer waveguides was 6.5 cm. The outer rods were welded to a thin (2 mm) metal bar, and the inner rod soldered to a 50 ohm BNC connector; the entire handle was encased in epoxy resin. The cable length was 1 m. Measurements were taken during the summer of 1995 on two soils that had contrasting textures, a silty clay loam and a loamy sand. The silty clay loam soil is classified as Beltsville silt loam. The loamy sand soil is Rumford loamy sand. The data collection process was as follows. The TDR waveguides were inserted into the soil and a measurement recorded. Then, a soil coring device 10 cm in diameter and 10 cm long was used to extract an undisturbed

Table 1. Values of water contents, the corresponding apparent dielectric constant (K_a) obtained from the three methods, and the simulated characteristic impedance (Z_0) of the waveguides for the silty clay loam soil.

θ	$K_a^{0.5}$			Z_0
	Manual	Derivative-based	Simulated	
$m^3 m^{-3}$				
0.174	2.57	2.64	2.56	194.5
0.183	2.60	2.73	2.68	204.1
0.226	2.80	2.98	2.96	213.6
0.239	3.26	3.47	3.52	237.5
0.245	2.80	2.93	2.88	197.6
0.256	3.06	3.19	3.20	220.8
0.263	3.17	3.27	3.25	191.5
0.276	3.31	3.49	3.27	162.6
0.278	3.60	3.76	3.69	207.9
0.281	3.54	3.59	3.48	195.9
0.303	3.31	3.57	3.40	194.8
0.313	3.37	3.58	3.21	155.1
0.316	3.57	3.82	3.76	215.6
0.317	3.54	3.68	3.64	213.9
0.398	4.23	4.37	3.88	161.5
0.411	4.17	4.38	3.96	182.9
0.417	4.29	4.55	4.16	175.7
0.429	4.37	4.57	4.16	185.8
0.433	4.80	4.83	4.32	160.9

Table 2. Values of water contents, the corresponding apparent dielectric constant (K_a) obtained from the three methods, and the simulated characteristic impedance (Z_0) of the waveguides for the loamy sand soil.

θ	$K_a^{0.5}$			Z_0
	Manual	Derivative-based	Simulated	
$m^3 m^{-3}$				
0.078	1.57	1.70	1.72	216.3
0.082	1.74	1.82	1.82	226.8
0.098	1.63	1.77	2.02	282.0
0.100	1.91	2.11	1.91	210.0
0.100	1.97	2.10	1.99	216.2
0.103	1.89	2.04	1.61	173.2
0.104	1.83	1.94	1.88	216.3
0.105	1.86	1.92	1.92	252.5
0.110	1.94	2.09	1.83	197.7
0.111	2.03	2.14	1.96	202.1
0.112	2.06	2.17	1.95	209.7
0.115	2.06	2.24	2.08	222.7
0.137	2.17	2.40	2.03	203.2
0.143	2.23	2.51	2.31	232.9
0.151	2.40	2.53	2.35	246.0
0.153	2.29	2.53	2.32	228.2
0.154	2.23	2.40	2.28	241.6
0.158	2.31	2.49	2.12	210.7
0.163	2.23	2.50	2.42	256.1
0.166	2.31	2.57	2.49	240.1
0.166	2.23	2.35	2.42	257.5
0.214	2.83	3.01	3.12	255.3
0.227	2.80	2.96	3.26	254.6
0.236	3.03	3.20	3.28	239.7
0.259	3.20	3.37	3.28	246.6
0.286	3.71	3.86	3.80	241.9
0.287	3.60	3.78	3.72	243.7
0.288	3.37	3.55	3.68	255.8
0.301	3.71	3.86	3.72	220.3
0.318	3.83	3.99	3.96	236.7

soil core from an area surrounding the probe insertion point. Three TDR measurements and cores were collected at each sampling time for a total of 26 measurements for the silty clay loam soil and 30 measurements for the loamy sand soil. The soil was removed from the cores and dried for at least 48 h at 80°C.

Wave traces were recorded with a Tektronix 1502B cable tester with an RS232 serial port attached to a laptop computer. A program supplied by Tektronix for DOS-based computers, SP.EXE, was used to transfer the waveforms to the laptop, and each trace consisted of 251 points. The SP.EXE program records data from the TDR screen as the number of pixels above the base of the screen. The x coordinates, x_i , (units of length) were calculated from the distance per division setting which was set to 0.1 m. Since each division on the Tektronix 1502B is 25 pixels wide, $\Delta x = 0.1/25$ or 0.004 m for this setting. Voltage was obtained from the pixel height (y_i) recorded by the TDR instrument as $V = (V_0) (\text{gain}) + (y_i - y_1)/PR$. Here V_0 is the initial voltage of the TDR (0.3 v), y_i is the pixel height at x_i , gain is the voltage amplification factor to scale the waveform, PR is the ratio of pixels to voltage and is adjusted for each waveform to produce a final voltage that is two times the initial voltage, and y_1 is a baseline voltage calculated from the mean of the first five values of pixel height. Time at position, x_i , was calculated as

$$t_i = \frac{2x_i}{c} \tag{11}$$

where c is the speed of light. The time interval for simulations, Δt , was calculated as $\Delta t = 2\Delta x/c$ (V_p was set at 0.99).

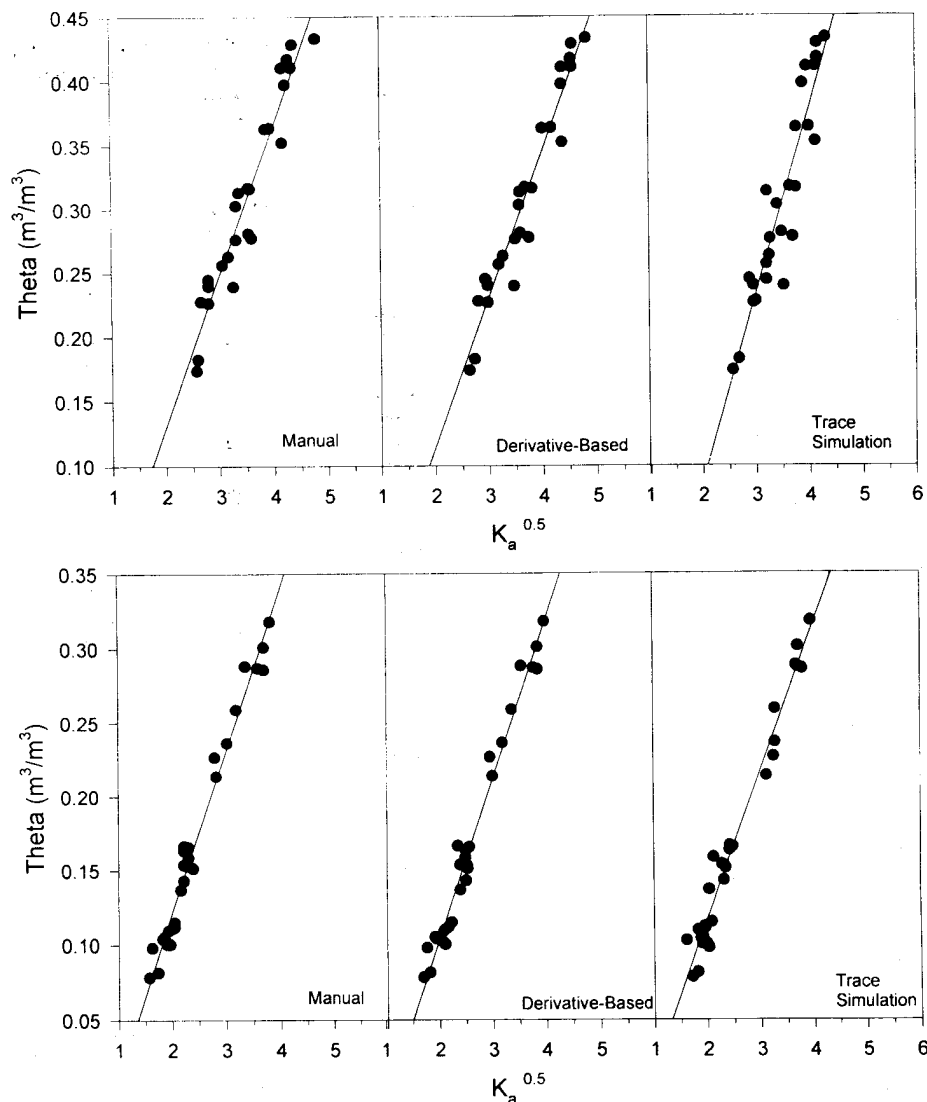


Fig. 6. Calibration curves for the three methods of time domain reflectometry calibration for two soils: (a) silty clay loam and (b) loamy sand (K_a = dielectric constant).

RESULTS AND DISCUSSION

The performance of the trace simulation method was greatly improved by the introduction of the correction for the inertia of the instrument (Fig. 5). The average mean square deviation between measured and calculated voltages was $<0.035 V$ in 95% of all cases. The shapes of the traces were also similar to the shapes of measured ones (Fig. 5). The values of $K_a^{0.5}$ output by the simulation program were not very different from $K_a^{0.5}$ obtained directly from the wave traces for both soils (Tables 1 and 2). This suggests that the simulation method yields realistic values of K_a .

The relationships between the measured water contents and $K_a^{0.5}$ for the three methods are in Fig. 6. The water contents and calculated values of $K_a^{0.5}$ are in Tables 1 and 2. The linear dependence

$$\theta = b_1 + b_2 \sqrt{K_a} \quad [12]$$

where b_1 and b_2 are parameters fit to the data for all three methods. The fitted parameters and descriptive

statistics are in Table 3. The relative differences between the intercepts and slopes of the fitted relationships for the loamy sand and silty clay loam in Table 3 are similar to those in equations reported by Heimovaara (1993). The derivative-based method gave the best results; it had the smallest standard error for both soils ($0.0194 \text{ m}^3 \text{ m}^{-3}$ for the silty clay loam and $0.0115 \text{ m}^3 \text{ m}^{-3}$ for the loamy sand). The manual method provided the next best calibration, and the wave simulation method resulted in the lowest precision (Table 3). These standard errors reflect the spatial variability of soil properties and water content variations within the core and the intrinsic uncertainties of the methods used to obtain K_a . The error was higher for the silty-clay soil than for the sandy soil. Similar results for fine- and coarse-textured soils were reported by Topp et al. (1980) for their Rubicon (sandy, mixed, frigid Entic Haplorthod) and Bainsville [fine-silty, mixed (calcareous), mesic Ustic Torriorthent] soils. An uneven distribution of water in the silty-clay soil as

Table 3. Statistics and regression coefficients of the three trace analysis methods for the two soils.

Calibration method	Calibration equation†				Performance parameters‡	
	Intercept		Slope		s_e	r
	b_1	s_{b1}	b_2	s_{b2}		
Silty clay loam						
Manual	-0.102	0.0234	0.1167	0.0065	0.0212	0.930
Derivative-based	-0.1143	0.0220	0.1147	0.0059	0.0194	0.940
Trace simulation	-0.2013	0.0405	0.1448	0.01144	0.0287	0.869
Loamy sand						
Manual	-0.0972	0.0082	0.1088	0.0033	0.01189	0.975
Derivative-based	-0.1108	0.0085	0.1072	0.0032	0.01159	0.976
Trace simulation	-0.0821	0.0083	0.0995	0.0032	0.0125	0.972

† b_1 and b_2 = estimates of the intercept and slope of the linear regression of water content on the apparent soil dielectric constant, s_{b1} and s_{b2} = standard errors of the estimated parameters.

‡ s_e = standard error, r = correlation coefficient.

opposed to the sandy soil may have contributed to the higher error.

There were no significant differences among the slopes and intercepts of the calibration functions for the derivative and manual methods for either soil (Table 4). The slopes and intercepts from the manual and derivative-based methods were nearly identical. At a significance level of 0.05, the slopes and one intercept of the simulation method were different from those for the manual and derivative methods for the silty-clay soil. Only the intercepts of the derivative and simulation methods were different at a significance level 0.05 for the sandy soil, however. None of the differences were significant at a probability level of 0.01. The use of an incorrect probe constant in the derivative method is a potential source of bias that would result in a different intercept compared with the manual method. The relative error, however, would decrease as the waveguide length increased. We did not see any evidence for that kind of bias in these data, however.

The fitted impedances (Z_0) for the waveguides are listed in Tables 1 and 2. The average value of the impedance, Z_0 , for the waveguides in soil was 198 Ω and the standard deviation was 24 Ω for the silty-clay soil. The value for the sandy soil was 231.4 Ω with a standard deviation of 22.3 Ω . The theoretical value for an ideal line in air can be calculated from $60 \ln(b/a)$ (Zegelin et al., 1989). Here b is the distance between the two outer rods and a is the diameter of the rod for a balanced probe design with three waveguides. This equation gave a value of 178.3 Ω that was smaller than the average of the estimates for either the sand or the clay. Zegelin et al. (1989) also found measured values of the characteristic impedance (Z_0) to be higher than those calculated by the geometric equation. They attributed the difference to deviation of the geometry from that of an ideal coaxial line. This and the fact that the wave simulation gave values of the dielectric constant

similar to the other methods suggest that the fitted impedances are realistic.

In our first set of simulations, we obtained an average value of the characteristic inertia time, λ , of 0.27 ns with standard deviation 0.07 ns for both soils. The rise time for the 1502B Tektronix TDR is ≈ 0.20 ns and is close to the estimate of mean λ . However, λ is still a lumped parameter accounting for other sources of dispersion. The rise time may also increase at longer cable lengths (Heimovaara, 1993). Therefore, in practice, a new value of λ may be needed as cable length changes. This mean value of λ was used in the simulations to determine the values of K_a and Z_0 given in Tables 1 and 2.

There are several reasons for the higher variability of water content estimates given by the wave simulation method. The theory on which the model is based does not account for all the phenomena that occur in a transmission line surrounded by a conductive dielectric medium (Yanuka et al., 1988). Another factor is the relatively short length of the handle that is near the limits of resolution of the Tektronix 1502B cable tester. This may result in somewhat greater uncertainty for the fitted parameters. There was an added level of variability because of having to fit a relatively large number of parameters (four). In addition to the slightly higher error, another disadvantage of the simulation method is that it requires more processing time than the derivative method. The method, however, could be improved by adding parameters to account for attenuation of the wave trace. The intercept and slope of the calibration function from the simulation method, however, were not greatly different from those derived from the other two methods. Overall, the simulated wave traces fit the measured traces reasonably well, and the parameters were physically meaningful. For this reason, wave trace simulation may be useful in studies of theoretically based calibration. The simulation method can also be a useful alternative

Table 4. Comparison of slopes and intercepts for the three methods.

Source	Loamy sand				Silty clay loam			
	Intercept		Slope		Intercept		Slope	
	t value	Probability	t value	Probability	t value	Probability	t value	Probability
Manual vs. derivative	1.13	0.262	0.35	0.729	0.34	0.738	0.186	0.853
Manual vs. simulation	2.89	0.196	2.06	0.423	2.35	0.213	2.35	0.021
Derivative vs. simulation	2.43	0.017	1.71	0.090	2.04	0.045	2.54	0.013

to the other two methods for wave trace analysis and may also hold promise as a method to calculate water contents in discrete layers where TDR probes are installed vertically.

SUMMARY AND CONCLUSIONS

We compared three methods to obtain K_a for TDR calibration, a manual method, a derivative-based algorithm, and fitting of the simulated trace to a measured one. For the simulation method, a model of the characteristic inertia that approximates the rise time of the cable tester has been introduced. Apparent dielectric constants (K_a) for 10-cm probes inserted from the soil surface were measured with a Tektronix 1502B cable tester. Water contents were obtained from soil cores taken from two soils with contrasting textures, a loamy sand and a silty clay loam. A linear regression of $K_a^{0.5}$ and water content was used to describe the relationship between water content and K_a for water contents between 0.08 and $0.43 \text{ m}^3 \text{ m}^{-3}$ for all three methods. The automated, derivative-based method gave the best results for both soils. The differences, among the three methods, however, were not large. The standard errors for the three methods in the silty clay loam soil were $0.019 \text{ m}^3 \text{ m}^{-3}$ for the derivative-based method, $0.0212 \text{ m}^3 \text{ m}^{-3}$ for the manual method, and $0.0287 \text{ m}^3 \text{ m}^{-3}$ for the wave simulation method. The standard errors in the loamy sand soil were $0.0118 \text{ m}^3 \text{ m}^{-3}$ for the derivative-based method, $0.0115 \text{ m}^3 \text{ m}^{-3}$ for the manual method, and $0.0125 \text{ m}^3 \text{ m}^{-3}$ for the simulation method. The relative differences between the parameters for the calibration equations for the fine-textured and coarse-textured soils were similar to those given in Heimovaara (1993) for soils with similar textures.

Wave simulations fit the measured data well enough to make it a useful technique to obtain apparent K_a from TDR wave traces. The simulation method gave a realistic estimate of the intrinsic impedance (Z_0) for the waveguides. The simulation method also gave a value of the characteristic inertia (λ) that was close to the rise time of the Tektronix 1502B cable tester. Because the parameters are physically based, this method of wave trace simulation may be useful in studies of theoretically based calibration. The disadvantages are that it requires longer processing time and results in a slightly different calibration equation.

We compared several methods of trace analysis that used the same reference point to locate the start of the travel time calculation, i.e., the location of the point where the waveguides entered the soil. There were slight differences in calibrations obtained for the three different methods. The reference point may not always correspond to the location of the soil-handle boundary, however. The equation of Ledieu et al. (1986), which is widely used, was based on a trace analysis method that used, as a reference, an impedance mismatch generated by diodes located in the region of handle. Their reference point, therefore, was somewhere in the handle and not at the handle-soil boundary. Because they used relatively long probes, the relative error of this offset was likely to be small and would affect only the intercept of the calibration equation. There are a number of ways to locate the initial inflection (a short summary is given in

Heimovaara, 1993). Cable length can also affect the calibration parameters by degrading the ability to accurately detect the initial and final reflections (Heimovaara, 1993). This suggests that error can be minimized when using a published calibration curve if the user has knowledge of how the estimate of K_a was obtained from the travel time and the type of probes and probe constants that were used. Finally, an automated method of determining K_a may result in lower error of predicted water contents as opposed to a manual method.

ACKNOWLEDGMENTS

The authors thank Dr. John Baker and Dr. Kevin O'Connor for their helpful suggestions after they reviewed an earlier draft of this paper.

REFERENCES

- Baker, J.M., and R.R. Allmaras. 1990. System for automating and multiplexing soil moisture measurement by time-domain reflectometry. *Soil Sci. Soc. Am. J.* 55:1-6.
- Baker, J.N., and R.J. Lascano. 1989. The spatial sensitivity of time-domain reflectometry. *Soil Sci.* 147:378-384.
- Dalton, F.N., and M.Th. van Genuchten. 1986. The time domain reflectometry method for measuring soil water content and salinity. *Geoderma* 38:237-250.
- Dasberg, S., and J.W. Hopmans. 1992. Time domain reflectometry calibration for uniformly and nonuniformly wetted sandy and clayey loam soils. *Soil Sci. Soc. Am. J.* 56:1341-1345.
- Dirksen, C., and S. Dasberg. 1993. Improved calibration of time domain reflectometry soil water content measurements. *Soil Sci. Soc. Am. J.* 57:660-667.
- Dobson, M.C., F.T. Ulaby, M.T. Hallikainen, and M.A. El-Rayes. 1985. Microwave dielectric behavior of wet soil: II. Dielectric mixing models. *IEEE Trans Geosci. Remote Sens.* GE-23:35-46.
- Heimovaara, T.J. 1993. Design of triple-wire time domain reflectometry probes in practice and theory. *Soil Sci. Soc. Am. J.* 57:1410-1417.
- Herkelrath, W.N., S.P. Hamburg, and F. Murphy. 1991. Automatic, real-time monitoring of soil moisture in a remote field area with time domain reflectometry. *Water Resour. Res.* 27:857-864.
- Jakobsen, O.H., and P. Schønning. 1993a. A laboratory calibration of time domain reflectometry for soil water measurement including effects of bulk density and texture. *J. Hydrol.* 151:147-157.
- Jakobsen, O.H., and P. Schønning. 1993b. Field evaluation of time domain reflectometry for soil water measurements. *J. Hydrol.* 151:159-172.
- Knight, J.H. 1992. The sensitivity of time domain reflectometry measurements to lateral variations in soil water content. *Water Resour. Res.* 16:574-582.
- Ledieu, J., P. de Ridder, P. de Clerk, and S. Dautrebande. 1986. A method of measuring soil moisture by time-domain reflectometry. *J. Hydrol.* 88:319-328.
- Neter, J., and W. Wasserman. 1974. *Applied linear statistical models.* Richard D. Irwin, Inc. Homewood, IL.
- SAS Institute. 1985. *SAS/STAT guide for personal computers.* Version 6 ed. SAS Inst., Cary, NC.
- Spaans, E.J.A., and J.M. Baker. 1993. Simple baluns in parallel probes for time domain reflectometry. *Soil Sci. Soc. Am. J.* 57:668-673.
- Topp, G.C., J.L. Davis, and A.P. Annan. 1980. Electromagnetic determination of soil water content: Measurements in coaxial transmission lines. *Water Resour. Res.* 16:574-582.
- Topp, G.C., J.L. Davis, and A.P. Annan. 1982. Electromagnetic determination of soil water content using TDR: I. Applications to wetting fronts and steep gradients. *Soil Sci. Soc. Am. J.* 46:672-678.
- van Genuchten, M.Th. 1981. Non-equilibrium transport parameters from miscible displacement experiments. U.S. Salinity Lab. Research Rep. 119, USDA-SEA-ARS, Riverside, CA.
- Yanuka, M., G.C. Topp, S. Zegelin, and W.D. Zebchuk. 1988. Multiple reflection and attenuation of time-domain reflectometry pulses: Theoretical considerations for applications to soil and water. *Water Resour. Res.* 7:939-944.
- Zegelin, S.J., I. White, and D.R. Jenkins. 1989. Improved field probes for soil water content and electrical conductivity measurements using TDR. *Water Resour. Res.* 25:2367-2376.